Oxygen-broadened and air-broadened linewidths for the NO infrared absorption bands by means of the exact-trajectory approach

J. Buldyreva,* S. Benec'h, and M. Chrysos
Laboratoire des Propriétés Optiques des Matériaux et Applications, Unité Mixte de Recherche, CNRS UMR No. 6136, Université d'Angers, 2 Boulevard Lavoisier, 49045 Angers, France
(Received 14 September 2000; published 6 February 2001)

Semiclassical *ab initio* values of oxygen-broadened and air-broadened NO infrared linewidths are reported in the range of atmospheric temperatures 163–299 K. The calculation is based on the authors' recently developed extended exact trajectory approach implemented within the Robert-Bonamy formalism for collisional line broadening. The results obtained are found to be in excellent agreement with recent straightforward measurements.

DOI: 10.1103/PhysRevA.63.032705 PACS number(s): 34.10.+x, 33.70.Jg

I. INTRODUCTION

During the last decades the nitric monoxide infrared absorption has been extensively studied both experimentally and theoretically. The motivation for undertaking such studies is the abundance of NO in the upper Earth's atmosphere. Stratospheric injections and aircraft emissions are two examples among a variety of NO sources. In practice, measurements of the NO concentration require accurate data of linewidths, intensities, and line positions, over a wide range of temperatures and pressures for different perturbers. Two of the most important perturbing species are nitrogen and oxygen since they are the main constituents of the air.

Given that experimentation with NO-N_2 is quite easily feasible, the need for a better understanding—from the theoretical standpoint—of the structure and dynamics of this system through a meaningful comparison with the experiment appeared very early, and semiclassical studies of NO-N_2 had been attempted already in the 1970s [1–4]. In spite of the advent of high-speed computers, semiclassical approaches are still preferable as compared to straightforward quantum-mechanical computations because of the complexity of the aforementioned system. In this context, it turns out that Robert and Bonamy's (RB) [5] theory is the most advanced of all semiclassical approaches thus far developed. However, because it uses parabolic trajectories (PT) to describe the relative motion of two colliding molecules, this formalism is known to provide inaccurate linewidths for high values of the rotational quantum number [2]. Recently, we proposed a more rigorous methodology for symmetric top active molecules [6] based on the exact trajectory (ET) approach [7,8] and implemented within the RB formalism. A good agreement with the experiment was found for both $^2\Pi_{1/2}$ and $^2\Pi_{3/2}$ subbands in the temperature range 163–296 K. We thus managed to substantially improve the theoretical values of the literature, and this enabled us to complete data for NO for temperatures which were unstudied until that time [6].

In the present paper we are rather focusing on an analogous but complementary study involving oxygen-broadened NO infrared linewidths. The high reactivity of O_2, which readily reacts with NO to form NO_2 through the reaction $2\,NO + O_2 \rightarrow 2\,NO_2$, had for a long time inhibited experimentalists to make straightforward measurements. In fact, so far, the only way to assess the role of oxygen as a perturber was through theoretical analyses. However, such estimates suffer from the lack of reliability and rigor because of the arbitrariness in the way to parametrize the NO-O_2 intermolecular potential surfaces in conjunction with the *a priori* unknown degree of validity of the theoretical results which strongly depend on the response of the model used.

Only very recently some experimental data for NO-O_2 linewidths at 299 K [9] and 295 K [10] became available, by two research groups independently. The experiment of Chackerian *et al.* [9] dealt with the fundamental band and was held in an environment of oxygen of constant pressure. A particular experimental setup was for this purpose elaborated, which made use of a flow system to eliminate the buildup of NO_2 and to replace the concentration of NO. The second experiment, that by Allout *et al.* [10], dealt with the first overtone band; the partial pressure of NO incide the cell decreased during the recording of the interferogram. A special method was used therein to obtain collisional widths from Fourier-transform spectra. The experimental data reported by these two groups may therefore serve as a reference for making useful comparisons with theoretical results to be reported here, ending up with rigorous predictions of broadening coefficients for NO perturbed by the air.

As far as theoretical results are concerned, the first calculation of linewidths for the aforementioned systems was held by Tejwani *et al.* [1] in the framework of the Anderson-Tsao-Curnutte (ATC) theory [12,13], but their approach was invalid for nonpolar molecules (N_2 and O_2) and led to unsatisfactory results. Later on, a more rigorous computation was carried out by Houdeau *et al.* [2] within the RB formalism using parabolic trajectories, and theoretical data based on their results have been included in the HITRAN96 database for NO pertubed by air [11]. It should, however, be pointed out that the latter information is very approximate, the reported values being identical for all lines (see the footnote of Table 2 of Ref. [11]).

Our paper is organized as follows. In Sec. II we briefly

*Email address: jeanna.buldyreva@univ-angers.fr

TABLE I. Physical parameters characterizing the intermolecular potential NO-O_2; atomic Lennard-Jones parameters are given for the three available parametrizations: low limit (I), midpoint (II), and high limit (III).

d_{ij} [a] (erg Å^{12})	e_{ij} [a] (erg Å^{6})	$\lvert r_{1i}\rvert,\lvert r_{2j}\rvert$ [a] (Å)	Q [b] (10^{-26} esu) μ (10^{-18} esu)	B_0 [c] (cm^{-1})
$d_{N\text{-}O}=0.1424$ (I)	$e_{N\text{-}O}=0.1910$ (I)			
$d_{O\text{-}O}=0.0673$ (I)	$e_{O\text{-}O}=0.1459$ (I)			
$d_{N\text{-}O}=0.2547$ (II)	$e_{N\text{-}O}=0.2502$ (II)	$\lvert r_{1N}\rvert=0.614$	$Q_{NO}=-1.8$	$B_{0NO}=1.6957$
$d_{O\text{-}O}=0.1326$ (II)	$e_{O\text{-}O}=0.1980$ (II)	$\lvert r_{1O}\rvert=0.537$	$Q_{O_2}=-0.39$	$B_{0O_2}=1.4377$
$d_{N\text{-}O}=0.4286$ (III)	$e_{N\text{-}O}=0.3185$ (III)	$\lvert r_{2O}\rvert=0.603$	$\mu_{NO}=0.158$	
$d_{O\text{-}O}=0.2479$ (III)	$e_{O\text{-}O}=0.2606$ (III)			

[a]Reference [19].
[b]Reference [2].
[c]Reference [11].

present the features of the RB formalism adapted to the case of NO viewed as a symmetric top active molecule, and we recall the essential points of the ET approach. In Sec. III, the latter approach is applied to the calculation of oxygen-perturbed NO linewidths, for both $^2\Pi_{1/2}$ and $^2\Pi_{3/2}$ electronic subbands and for various temperatures ranging from 299 to 163 K. Then, the NO-O_2 results are combined with analogous data, recently provided by the authors for NO-N_2 [6], so that the air-broadening coefficients for the atmospheric constitution are calculated. In Sec. IV the main results are summarized and some perspectives are given.

II. THEORETICAL TREATMENT

Because of an unpaired electron, nitrogen monoxide is an intriguing and particulary challenging diatomic molecule. In

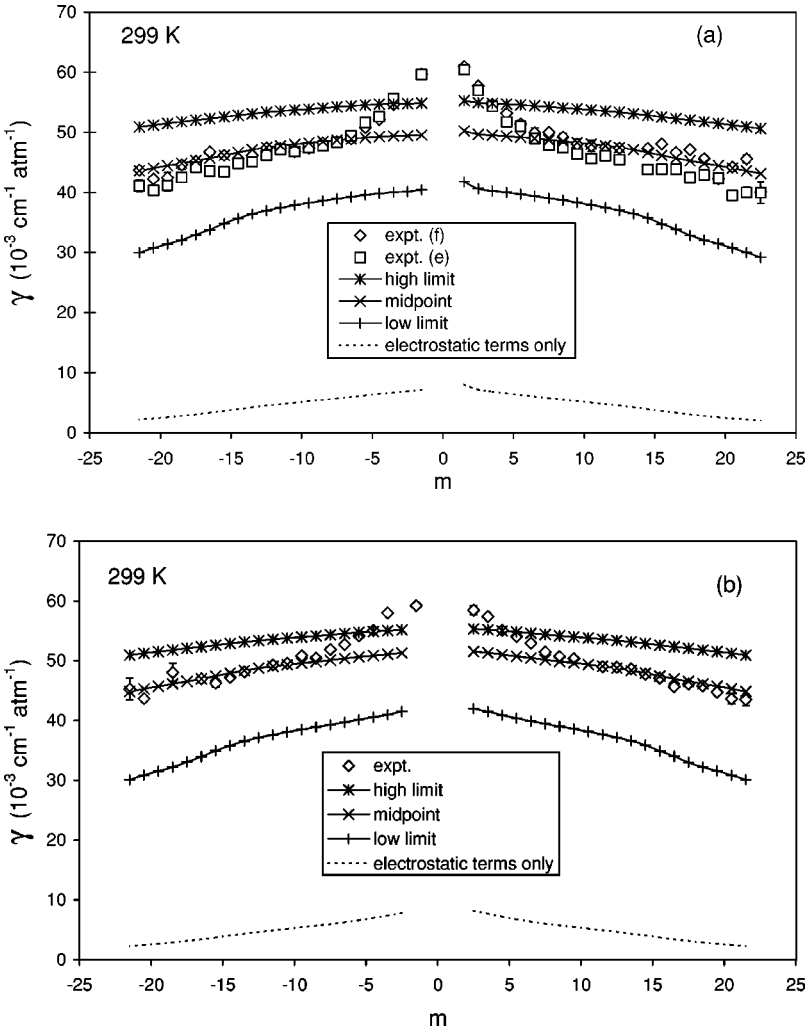

FIG. 1. Comparison between theoretical O_2-broadened NO linewidths for different parametrizations of the atom-atom potential (this work) and experimental data of Chackerian *et al.* [9] at 299 K: (a) $^2\Pi_{1/2}$ subband, *f* and *e* designate Λ-doubling components; (b) $^2\Pi_{3/2}$ subband.

contrast to ordinary diatoms, its ground electronic state is of a $^2\Pi$ type and splits up into two components, namely $^2\Pi_{1/2}$ and $^2\Pi_{3/2}$, via spin-orbit interaction. The corresponding rotational wave functions are those of a symmetric top, $|JKM\rangle$, characterized by a rotational quantum number J, a magnetic one M, as well as by an additional quantum number K, which designates the projection of the total angular momentum on the internuclear axis. The possible values of the latter quantum number are thus defined by the sum of the corresponding components of spin ($\Sigma = \pm 1/2$) and of electronic ($\Lambda = 1$) angular momenta: $K = 1/2$ or $K = 3/2$. We recall that the case of linear molecules with a Σ-ground electronic state corresponds to $K = 0$. The effects of an additional Λ-doubling caused by the coupling between the rotation of the molecule and the orbital motion of the electrons can sometimes be observed experimentally for NO [4,9,10], but these effects are neglected in the context of the semiclassical formalism to be applied here.

In order to make the RB approach [5] (which was initially developed for linear molecules in the ground Σ state) applicable to the more general case of a symmetric top active molecule, an extension of the formalism is required.

A. The Robert-Bonamy formalism for a symmetric top active molecule

The approach proposed a couple of decades ago by Robert and Bonamy [5] constitutes an important leap ahead in semiclassical studies since it manages to significantly improve the well-known (but insufficient) ATC theory. This became possible by means of an exponential form of the scattering matrix (which now avoids the ambiguous cutoff procedure) and a more physical model of a curved trajectory (which now is a parabola) governed by the isotropic potential.

Within this approach, for the case considered here, the linewidth (in cm^{-1}) γ_{fi} associated to a radiative transition $f \leftarrow i$ is reduced to

$$\gamma_{fi} = \frac{n_b}{2\pi c} \sum_{j_2} \rho_{j_2} \int_0^\infty v f(v) dv \int_0^\infty 2\pi b db \{1 - [1 - S^{(L)}_{2,f2i2}] \times \exp[-(S_{2,f2} + S_{2,i2} + S^{(C)}_{2,f2i2})]\}. \quad (1)$$

Here n_b stands for the numerical density of the perturbing particles and ρ_{j_2} denotes their thermal population. For practical calculations, the integration over the relative velocity v with the Maxwell-Boltzmann distribution $f(v)$ is replaced by the mean thermal velocity $\overline{v} = \sqrt{8kT/\pi m^*}$ (T is the temperature and m^* is the reduced mass of the molecular pair). The integral over the impact parameter b is replaced by the integral over the distance of closest approach r_c (for more details, see Ref. [5]), where r_c and b are related with each other via the energy conservation condition

$$b/r_c = \sqrt{1 - V^*_{iso}(r_c)}.$$

The asterisk denotes the isotropic potential's reduced value defined by $V^*_{iso} = 2V_{iso}/m^* v^2$. As V_{iso} the Lennard-Jones form $V_{LJ}(r) = 4\varepsilon[(\sigma/r)^{12} - (\sigma/r)^6]$ is often taken, where the two parameters ε and σ designate the depth of the potential well and the radius of action of the repulsive forces, respectively.

Explicit expressions for the various second-order contributions S_2 in Eq. (1) are tedious and lengthy, and can be

TABLE II. O_2-broadening coefficients (in cm^{-1} atm^{-1}) for NO at 299 K; our exact trajectory (ET) values are given for the midpoint parametrization II.

m	$^2\Pi_{1/2}(f)$ Expt. [9]	$^2\Pi_{1/2}(e)$ Expt. [9]	$^2\Pi_{1/2}$ ET II	$^2\Pi_{3/2}$ Expt. [9]	$^2\Pi_{3/2}$ ET II
−1.5	59.67(78)	59.59(87)	49.54		
−2.5			49.43	59.21(5)	51.30
−3.5	54.59(33)	55.64(32)	49.39	57.97(40)	51.07
−4.5	52.10(45)	52.60(34)	49.29	55.07(33)	50.87
−5.5	50.79(58)	51.63(50)	49.12	54.20(23)	50.63
−6.5	48.90(59)	49.38(36)	48.92	52.70(37)	50.37
−7.5	48.43(27)	48.33(60)	48.70	51.88(33)	50.10
−8.5	48.27(39)	47.75(64)	48.48	50.44(21)	49.84
−9.5	47.38(47)	47.45(62)	48.24	50.85(22)	49.58
−10.5	46.78(59)	46.78(44)	48.01	49.56(20)	49.32
−11.5	47.31(36)	47.13(54)	47.75	49.31(22)	49.05
−12.5	47.40(47)	46.17(62)	47.47		48.76
−13.5	46.15(50)	45.07(53)	47.10	48.15(30)	48.38
−14.5	45.59(11)	44.83(10)	46.64	47.22(37)	47.92
−15.5	46.21(46)	43.43(68)	46.18	46.25(68)	47.46
−16.5	46.74(30)	43.53(34)	45.69	46.98(26)	46.96
−17.5	45.16(61)	44.15(15)	45.26		46.53
−18.5	44.59(74)	42.53(73)	44.86	48.05(150)	45.13
−19.5	42.45(83)	41.15(93)	44.46		45.72
−20.5	42.25(36)	40.35(67)	44.03	43.67(16)	45.29
−21.5	43.72(25)	41.13(94)	43.61	45.25(180)	44.86
1.5	60.93(40)	60.42(07)	50.23		
2.5	57.71(26)	56.98(25)	49.67	58.45(73)	51.55
3.5	54.65(40)	54.34(67)	49.51	57.41(10)	51.33
4.5	53.16(35)	51.69(47)	49.37	55.11(25)	51.04
5.5	51.38(63)	51.01(64)	48.19	54.06(26)	50.75
6.5	49.95(78)	48.96(63)	48.97	52.92(22)	50.45
7.5	50.00(30)	47.86(57)	48.74	51.46(35)	50.17
8.5	49.18(60)	47.44(41)	48.50	50.70(30)	49.89
9.5	48.03(77)	46.38(54)	48.27	50.35(27)	49.62
10.5	47.72(89)	45.62(64)	47.03		49.35
11.5	47.50(67)	46.10(17)	47.77	49.00(30)	49.07
12.5	47.37(65)	45.41(61)	47.48	48.91(28)	48.77
13.5			47.10	48.66(8)	48.38
14.5	47.30(40)	43.80(54)	46.65	47.73(10)	47.93
15.5	48.07(10)	43.88(03)	45.18	47.09(48)	47.46
16.5	46.65(33)	43.89(09)	45.70	45.65(40)	46.98
17.5	47.12(34)	42.46(40)	44.26	46.12(29)	46.53
18.5	45.63(46)	42.93(45)	44.87	45.80(13)	46.13
19.5	42.99(67)	42.38(23)	44.46	44.73(38)	45.73
20.5	44.21(53)	39.50(47)	44.05	43.62(85)	45.31
21.5	45.57(62)	40.02(91)	43.59	43.49(96)	44.85
22.5	40.06(17)	39.95(1.80)	43.14		

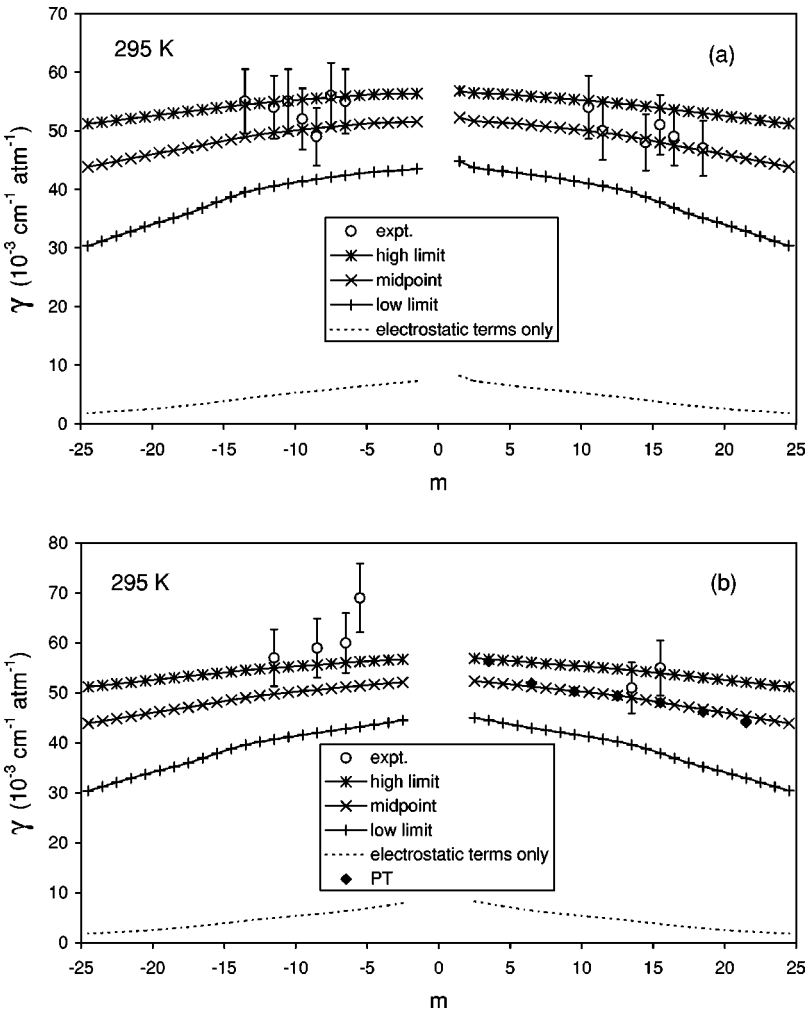

FIG. 2. Comparison between theoretical O_2-broadened NO linewidths for different parametrizations of the atom-atom potential (this work), midpoint values of Houdeau *et al.* [2] obtained with parabolic trajectory (PT), and experimental data of Allout *et al.* [10] at 295 K; (a) $^2\Pi_{1/2}$ subband, (b) $^2\Pi_{3/2}$ subband.

found in Ref. [5]. We simply note that all what is needed is matrix elements of the anisotropic potential V_{aniso} over rotational wave functions of the molecular system $|j_i m_i j_2 m_2\rangle$ before and after the collision. Under the classical path assumption, this function is factorized as a product of wave functions corresponding to the active molecule and to the perturber, so that the matrix element can be written as a product of separated matrix elements. When the active molecule no longer is linear, its wave functions, thus far spherical harmonics $Y_{lm}(\vartheta,\phi)$, have to be modified, and for the case of a symmetric top they have to be replaced by [14]

$$|JKM\rangle = \left(\frac{2J+1}{8\pi^2}\right)^{1/2} D^J_{-K,-M}(\psi,\vartheta,\phi). \qquad (2)$$

In Eq. (2), $D^l_{m'm}(\psi,\vartheta,\phi)$ are the Wigner rotation matrices (whose arguments have been reversed for practical purposes) described by the three Euler angles (ϕ,ϑ,ψ) relative to the orientation of the molecule in the laboratory-fixed frame.

When the anisotropic potential is represented by a series over anisotropy ranks of two interacting molecules l_1, l_2, the matrix element gives rise to the Clebsh-Gordan coefficients $C^{j'0}_{j0l_10}$ (for the collisional transition $j \rightarrow j'$) for a linear active molecule, and to $C^{j'K}_{jKl_10}$ in the case of a symmetric top. Note in passing that this modification, i.e., when switching from $K=0$ to $K\neq 0$, has already been implemented within a parabolic-shape trajectory and reported in the past [15], but no mathematical argumentation was made therein. A more detailed derivation has, however, been given throughout the presentation of our exact trajectory approach [6].

B. Exact trajectory approach

The exact solution of the classical equations of motion for a particle in the action of an isotropic potential is well known [16]. But only in 1992 was it proposed to incorporate it in a semiclassical calculation of spectral parameters [7,8]. It is noteworthy and somehow surprising, however, that in Refs. [7,8] this ET approach, conceived to provide high accuracies, was implemented within the ATC theory. Moreover, only lineshifts for some systems were calculated and reported therein, despite the fact that the degree of validity of this modeling should be checked more extensively by further applications. Last year, two such applications were made in the frame of the RB formalism for the vibrational line shifts of H_2-He [17] and for the isotropic linewidths of self-perturbed nitrogen [18]. In contrast to the preceding studies, where the active species were atoms or ordinary diatomic molecules, we managed to extend this approach to the case of a sym-

metric top active molecule and to apply it to the infrared linewidths of NO broadened by N_2 [6].

The main idea of the ET approach consists of using classical expressions for the time and phase of relative molecular motion as functions of the initial kinetic energy and the isotropic potential, aiming at replacing the integration of matrix elements over time by integration over intermolecular distances for a given value of the impact parameter (for more details, see Ref. [6]). Although the computational effort is much higher than that for analytical straight-line or parabolic trajectory expressions, a far better precision is attained provided that the potential employed is equally rigorous.

III. CALCULATION OF LINEWIDTHS

For NO-O_2 (as for NO-N_2), no *ab initio* potential-energy surface is available. Its anisotropic part V_{aniso} between two molecules 1 and 2 is thus represented as a superposition of long-range electrostatic interactions (dipole-quadrupole $V_{\mu_1 Q_2}$ and quadrupole-quadrupole $V_{Q_1 Q_2}$), as well as of atom-atom ones accounting for short-range forces,

$$V_{aniso}(r) = V_{el}(r) + V_{at\text{-}at}(r) = V_{\mu_1 Q_2} + V_{Q_1 Q_2} + \sum_{i,j} \left(\frac{d_{ij}}{r_{1i,2j}^{12}} - \frac{e_{ij}}{r_{1i,2j}^{6}} \right).$$

The summation is taken over the ith atoms of the first molecule and the jth atoms of the second molecule. The atomic pair energy parameters d_{ij}, e_{ij}, $r_{1i,2j}$ as well as the multipolar moments for the considered systems are listed in Table I. This expression for V_{aniso} is the same as that of Refs. [2,6] and enables us to realize a meaningful comparison of results obtained with different trajectories.

We first calculate the linewidths of NO embedded in an environment of oxygen. Different temperatures, ranging from 299 K down to 163 K, are studied, allowing us to check the applicability of our approach. Then, using the up-to-date NO-N_2 theoretical data from our previous work [6], we compute the broadening coefficients for NO perturbed by the air.

A. The NO-O_2 case

Let us start our analysis by the temperature of 299 K, for which a series of experimental linewidths by Chackerian *et al.* is available [9]. Since the optimal parametrization of the NO-O_2 potential is *a priori* unknown [19], computations are done against the quantum number m for the three parametrizations which are available: low-limit (I), midpoint (II), and high-limit (III) [19]; we recall that for the P branch, $m = -J$, while in the R branch it is $m = J+1$. Results are illustrated in Figs. 1(a) and 1(b). What is attested there is that the calculated linewidths strongly depend on the way to parametrize; therefore, a good estimation of the atom-atom parameters d_{ij}, e_{ij} is of crucial importance. For both $^2\Pi_{1/2}$ and $^2\Pi_{3/2}$ subbands, for not too low rotational numbers, the midpoint parametrization for the exact trajectory approach provides an excellent agreement with the experimental data; only for very low rotational numbers some deviation in the

TABLE III. O_2-broadening coefficients (in cm^{-1} atm^{-1}) for NO at 295 K; our exact trajectory approach (ET) values are given for the midpoint (II) and high-limit (III) parametrizations.

m	$^2\Pi_{1/2}$ Expt. [10]	$^2\Pi_{1/2}$ ET II	$^2\Pi_{1/2}$ ET III	$^2\Pi_{3/2}$ Expt. [10]	$^2\Pi_{3/2}$ PT [2]	$^2\Pi_{3/2}$ ET II	$^2\Pi_{3/2}$ ET III
−1.5		51.57	56.37				
−2.5		51.45	56.30			52.13	56.73
−3.5		51.37	56.26			51.89	56.58
−4.5		51.30	56.18			51.68	56.44
−5.5		51.12	56.04	69		51.44	56.25
−6.5	55	50.92	55.87	60		51.18	56.05
−7.5	56	50.69	55.70			50.89	55.84
−8.5	49	50.45	55.50	59		50.62	55.63
−9.5	52	50.20	55.31			50.35	55.42
−10.5	55	49.95	55.13			50.07	55.22
−11.5	54	49.68	54.94	57		49.78	55.01
−12.5		49.38	54.72			49.47	54.79
−13.5	55	48.97	54.46			49.06	54.52
−14.5		48.50	54.18			48.59	54.24
−15.5		48.03	53.89			48.11	53.94
−16.5		47.52	53.58			47.60	53.63
−17.5		47.07	53.30			47.15	53.35
−18.5		46.65	53.01			46.72	53.06
−19.5		46.21	52.70			46.28	52.74
−20.5		45.74	52.39			45.81	52.43
−21.5		45.27	52.08			45.33	52.12
−22.5		44.81	51.79			44.87	51.82
−23.5		44.31	51.49			44.37	51.53
−24.5		43.89	51.20			43.94	51.24
1.5		52.26	56.82				
2.5		51.69	56.45			52.38	56.90
3.5		51.52	56.34		56.3	52.16	56.75
4.5		51.38	56.23			51.85	56.55
5.5		51.20	56.08			51.56	56.33
6.5		50.96	55.90		51.9	51.26	56.10
7.5		50.73	55.71			50.97	55.88
8.5		50.48	55.52			50.67	55.66
9.5		50.23	55.33		50.3	50.39	55.44
10.5	54	49.97	55.14			50.10	55.24
11.5	50	49.69	54.94			49.81	55.03
12.5		49.38	54.72		49.4	49.48	54.80
13.5		49.97	54.46	51		49.07	54.52
14.5	48	49.51	54.18			48.60	54.24
15.5	51	49.03	53.89	55	48.1	48.12	53.95
16.5	49	47.53	53.58			47.61	53.64
17.5		47.07	53.30			47.15	53.35
18.5	47	46.65	53.01		46.2	46.72	53.06
19.5		46.21	52.70			46.28	52.74
20.5		45.75	52.40			45.82	52.44
21.5		45.28	52.09		44.1	45.34	52.13
22.5		44.78	51.79			44.85	51.82
23.5		44.33	51.49			44.39	51.53
24.5		43.87	51.20			43.92	51.24

TABLE IV. Comparison between theoretical values of NO-O_2 linewidths at 163 K; *R* branch of the $^2\Pi_{3/2}$ subband (parametrization II is employed in both approaches).

J	PT (Ref. [2])	ET (this work)
2.5	91.0	84.4
5.5	83.5	82.0
8.5	81.3	79.6
11.5	78.2	76.1
14.5	74.1	72.8
17.5	69.7	69.2
20.5	65.2	65.9

trend is observed (for numerical values see Table II). We ascribe the inability of the ET approach to predict accurate linewidths for small *J* to the roughness of the atom-atom parameters. Indeed, for the system considered, the long-range electrostatic interactions are very weak: $\mu_1 = 0.158 \times 10^{-18}$ esu and $Q_2 = -0.39 \times 10^{-26}$ esu, the latter value to be compared with $Q_2 = -1.59 \times 10^{-26}$ esu for NO-N_2. Hence, in opposition to NO-N_2 where the linewidths for small *J* are mainly due to electrostatic interactions [15,2,6], the corresponding contributions for NO-O_2 no longer are dominant (dashed curves on Fig. 1) and, therefore, no more are they able to give rise to the characteristic ''shoulder'' [20,6]. The role of short-range forces are thus very important for these rotational numbers and a slightly inaccurate parametrization may remove all advantages of the (sensitive) exact trajectory approach.

Another series of experimental data (with uncertainties of about 10%) was obtained by Allout *et al.* at 295 K [10]. These data are plotted together with our corresponding theoretical values (for parametrizations I–III) in Fig. 2. In addition, for the $K = 3/2$ case [Fig. 2(b)] available theoretical results of Houdeau *et al.* [2], obtained with parabolic-shape trajectories with parametrization II, are also included. Table III gathers all numerical values. For the diamagnetic subband, Fig. 2(a) shows that for the *R*-branch ($m > 0$) linewidths the midpoint parametrization remains preferable but for the *P* branch ($m < 0$) the high-limit parametrization seems to work better. The same tendency is observed for the paramagnetic subband, as well [Fig. 2(b)]. It should also be stressed that the predictions of the PT approach are almost identical to our ET results, both obtained with parametrization II. Only slight deviations are observed at extreme values (both low and high) of the rotational quantum number. This tendency of the parabolic trajectory approach to provide

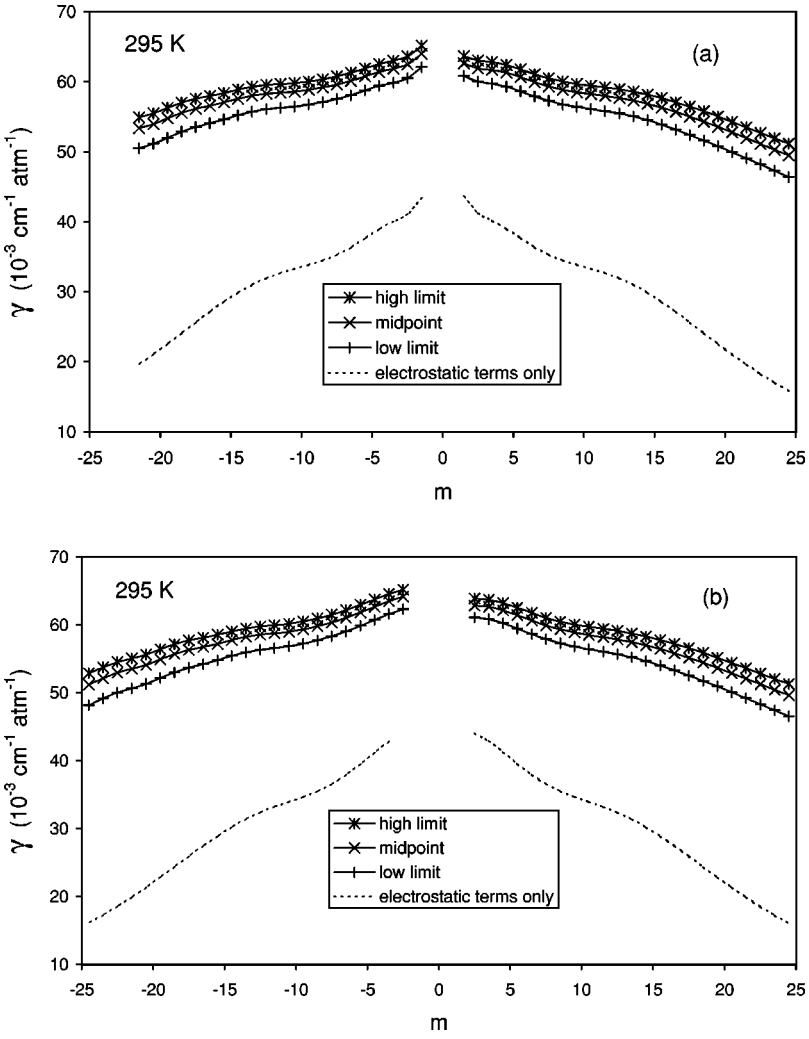

FIG. 3. Comparison between theoretical air-broadened NO linewidths for different parametrizations of the NO-O_2 atom-atom potential (this work) at $T = 295$ K: (a) $^2\Pi_{1/2}$ subband, (b) $^2\Pi_{3/2}$ subband.

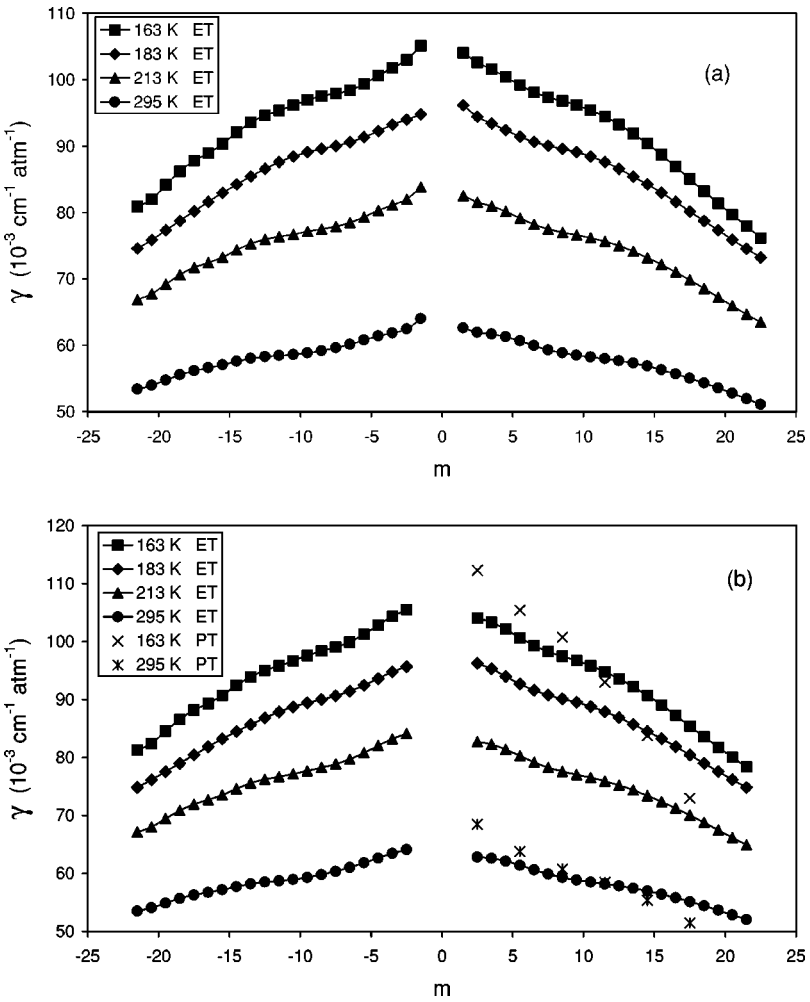

FIG. 4. Temperature dependence of air-broadened NO linewidths calculated with the exact trajectory (ET) approach (midpoint parametrization for NO-O_2) and analogous results obtained with the parabolic trajectory (PT) approach [2]: (a) $^2\Pi_{1/2}$ subband, (b) $^2\Pi_{3/2}$ subband.

larger linewidths for small J while smaller ones for large J in comparison to the exact trajectory ones, has already been reported [18,6] and should be recognized as a signature of the two compared approaches.

For other temperatures, no experimental values for the oxygen-broadened NO linewidths are available, but some calculations have been performed by Tejwani *et al.* [1] and by Houdeau *et al.* [2]. As was mentioned above, the values of Ref. [1] are unsatisfactory and therefore there is no interest for these results to be reproduced. So, in Table IV we report our ET results together with the PT values of Ref. [2] for 163 K (midpoint parametrization). It can be stated from Table IV that the linewidths obtained with both trajectory approaches are very close to each other. Only some differences are again observed for very small rotational quantum numbers.

B. The NO-air case

Having already computed the line-boadening coefficients of NO for both perturbers, namely $\gamma_{\text{NO-N}_2}$ and $\gamma_{\text{NO-O}_2}$, the air-broadened linewidths are deduced by the simple weighting expression,

$$\gamma_{\text{NO-air}} = 0.79\,\gamma_{\text{NO-N}_2} + 0.21\,\gamma_{\text{NO-O}_2},$$

since, within binary collision regime, a single NO molecule is either perturbed by a N_2 molecule or by an O_2 one, whose concentrations in the atmosphere are of 79% and 21%, respectively, and the linewidth is an additive spectral property.

Aiming to analyze the influence of the different atom-atom NO-O_2 parametrizations on $\gamma_{\text{NO-air}}$, we plot in Fig. 3 ($^2\Pi_{1/2}$ and $^2\Pi_{3/2}$ subbands) the corresponding linewidths for 295 K; we note that for the NO-N_2 case the low-limit parameters were found to be more appropriate for modeling the experimental data. Due to the dominant concentration of N_2 in the atmosphere, the general tendency of the theoretical curves is analogous to that referring to the NO-N_2 case, but the electrostatic interactions (dashed line curve) are no longer dominant even when rotational numbers get small values. Furthermore, the ''shoulder,'' which thus far was observed in the $|m|$-values interval 5–15 [6], is now hardly reproduced. We also note that, despite the great differences between the parametrizations checked for NO-O_2, the air-perturbed linewidths are not of high sensitivity, relative deviations between theoretical results amounting to 2–3%.

Finally, in Fig. 4 the variation of the $\gamma_{\text{NO-air}}$ as a function of m, for different temperatures in the range 295–163 K, is

TABLE V. Comparison between theoretical values of NO-air linewidths; *R* branch of the $^2\Pi_{3/2}$ subband.

T	295 K		163 K	
J	PT (Ref. [2])	ET (this work)	PT (Ref. [2])	ET (this work)
2.5	68.5	64.3	112.3	103.3
5.5	63.8	62.3	105.4	99.3
8.5	60.8	60.5	100.8	96.7
11.5	58.5	59.5	93.0	93.6
14.5	55.4	57.9	83.8	89.0
17.5	51.5	55.8	73.0	83.6

plotted. Apart from Tejwani *et al.*'s work [1] for the *R* branch of the subband $^2\Pi_{1/2}$ at 300, 250, and 200 K and Houdeau *et al.*'s work [2] for the *R* branch of the subband $^2\Pi_{3/2}$ at 295, 250, 200, and 163 K, no other *ab initio* theoretical results have, to our knowledge, ever been reported for the temperature range considered. Analogously with the conclusions drawn for nitrogen and oxygen, these plots show that our air-broadening coefficients are substantially smaller than those of Houdeau *et al.* for low values of the rotational quantum number but greater for high ones. A straightforward numerical comparison is made in Table V.

IV. CONCLUSION

In this work the extended exact trajectory approach, recently developed by the authors [6], was applied to infrared line broadening. Linewidths for the fundamental band of NO perturbed by oxygen and air were *ab initio* calculated for different temperatures of atmospheric interest. This calculation significantly completed the scarce theoretical data which until the present work were available in the literature.

A straightforward comparison of our results for NO-O_2 with the experimetal values by Chackerian *et al.* [9] and Allout *et al.* [10] allowed us to make a detailed analysis of different ways to parametrize the atom-atom part of the interaction potential. In spite of the fact that the influence of the three different parametrizations on the oxygen-broadened linewidths was found to be strong, these parametrizations only weakly affect the linewidths for the air.

The results obtained with the exact trajectory once more clearly demonstrated the advantages of this approach, especially for the low temperatures for which the parabolic trajectory (PT) is inadequate. Given the fact that the use of a model interaction potential masked to a certain extent the subtleties of the approach, a more advanced study employing refined NO-O_2 and NO-N_2 potential surfaces whenever available would be of particular interest. This should allow us to draw definite conclusions on the degree of validity of our approach as well as on its accuracy.

[1] G. D. T. Tejwani, B. M. Golden, and E. S. Yeung, J. Chem. Phys. **65**, 5110 (1976).
[2] J. P. Houdeau, C. Boulet, J. Bonamy, A. Khayar, and G. Guelachvili, J. Chem. Phys. **79**, 1634 (1983).
[3] J. Ballard, W. B. Johnston, B. J. Kerridge, and J. J. Remedios, J. Mol. Spectrosc. **127**, 70 (1988).
[4] M. N. Spencer, C. Chackerian, Jr., L. P. Giver, and L. R. Brown, J. Mol. Spectrosc. **181**, 307 (1997).
[5] D. Robert and J. Bonamy, J. Phys. (Paris) **40**, 923 (1979).
[6] J. Buldyreva, S. Benec'h, and M. Chrysos, Phys. Rev. A **63**, 012 708 (2000).
[7] A. D. Bykov, N. N. Lavrent'eva, and L. N. Sinitsa, Atmos. Oceanic Opt. **5**, 587 (1992).
[8] A. D. Bykov, N. N. Lavrent'eva, and L. N. Sinitsa, Atmos. Oceanic Opt. **5**, 728 (1992).
[9] C. Chackerian, Jr., R. S. Freedman, L. P. Giver, and L. R. Brown, J. Mol. Spectrosc. **192**, 215 (1998).
[10] M.-Y. Allout, V. Dana, J.-Y. Mandin, P. Von Der Heyden, D. Décatoire, and J.-J. Plateaux, J. Quant. Spectrosc. Radiat. Transf. **61**, 759 (1999).
[11] A. Goldman, L. R. Brown, W. G. Schoenfeld, M. N. Spencer, C. Chackerian Jr., L. P. Giver, H. Dothe, C. P. Rinsland, L. H. Coudert, V. Dana, and J.-Y. Mandin, J. Quant. Spectrosc. Radiat. Transf. **60**, 825 (1998).
[12] P. W. Anderson, Phys. Rev. **76**, 647 (1949).
[13] C. J. Tsao and B. Curnutte, J. Quant. Spectrosc. Radiat. Transf. **2**, 41 (1962).
[14] R. P. Leavitt, J. Chem. Phys. **73**, 5432 (1980).
[15] J. Bonamy, A. Khayar, and D. Robert, Chem. Phys. Lett. **83**, 539 (1981).
[16] L. D. Landau and E. M. Lifshitz, *Mechanics*, 3rd ed., Course of Theoretical Physics Vol. 1 (Pergamon Press, Oxford, 1976).
[17] P. Joubert, J. Bonamy, and D. Robert, J. Quant. Spectrosc. Radiat. Transf. **61**, 19 (1999).
[18] J. Buldyreva, J. Bonamy, and D. Robert, J. Quant. Spectrosc. Radiat. Transf. **62**, 321 (1999).
[19] M. Oobatake and T. Ooi, Prog. Theor. Phys. **48**, 2132 (1972).
[20] J.-P. Bouanich and G. Blanquet, J. Quant. Spectrosc. Radiat. Transf. **40**, 205 (1989).